

RESEARCH PAPER

Development of an electrochemical aptasensor based on the gold nanorods and its application for detection of aflatoxin B1 in rice and blood serum samples

Mahmoud Roushani ^{1,*}, Behruz Zare Dizajdizi ¹, Zeinab Rahmati ¹, Azadeh Azadbakht ²

¹ Department of Chemistry, Ilam University, Ilam, Iran

² Department of Chemistry, Khorramabad Branch Islamic Azad University Khorramabad, Iran

ARTICLE INFO

Article History:

Received 27 November 2018

Accepted 10 February 2019

Published 15 June 2019

Keywords:

Aflatoxin B1

Aptasensor

Nanorod

Rice

ABSTRACT

Aflatoxins are a group of fungal mycotoxins produced mainly by molds; e.g., *Aspergillus flavus* and *Aspergillus parasiticus*. Among Aflatoxins, Aflatoxin B1 (AFB1) is the most toxic one. Therefore, there is a prompt need for determination of AFB1 in food products. This paper reports an electrochemical aptasensor for accurate determination of AFB1, which was constructed using gold nanorod sensing interface and aptamer as a specific recognition element. The synthesized gold nanorod was characterized by transmission electron microscopy, and the electrochemical behavior of fabricated aptasensor was investigated by cyclic voltammetry and electrochemical impedance spectroscopy. Under optimized conditions, the detection limit of the proposed aptasensor was 0.3 pM with dynamic range of 1.0 pM – 0.25 nM. This aptasensor represents a remarkable improvement in terms of sensitivity, selectivity, reproducibility and stability compared to the other methods for the determination of AFB1. This proposed sensor was successfully applied for the analysis of AFB1 in rice and blood serum samples.

How to cite this article

Roushani M, Zare Dizajdizi B, Rahmati Z, Azadbakht A. Development of an electrochemical aptasensor based on the gold nanorods and its application for detection of aflatoxin B1 in rice and blood serum samples. *Nanochem Res*, 2019; 4(1):35-42. DOI: 10.22036/ncr.2019.01.005

INTRODUCTION

Mycotoxins are secondary metabolites of molds that have contrary effects on humans, animals, and crops resulting in illnesses and economic losses. Contamination of food by mycotoxins is one of the most serious problems because the toxins are noxious to human and animal health [1, 2]. Aflatoxins are a group of fungal mycotoxins produced mainly by molds; e.g., *Aspergillus flavus* and *Aspergillus parasiticus* [3]. Among various kinds of aflatoxins, AFB1 is the most toxic, carcinogenic, mutagenic, and genotoxic one that grows on food crops during their production and storage [4, 5].

Various analytical techniques for AFB1 detection have been reported in the literature, such as high-performance liquid chromatography (HPLC), enzyme-link immunosorbent assay (ELISA), thin-layer chromatography (TLC) and electrochemistry [6-12]. Among the analysis methodologies mentioned, electrochemical techniques, because of their advantages including high sensitivity and selectivity, the stability of the response, low consumption of reagents and low cost, have gained a considerable attention as an alternative method of analysis [13, 14].

Aptamers are single-stranded DNA or RNA molecules that are chemically synthesized in vitro and capable of binding molecular targets from

* Corresponding Author Email: mahmoudroushani@yahoo.com
m.roushani@ilam.ac.ir

small molecules to proteins with high specificity and strong affinity [15-17]. Aptamer-based sensors have received a considerable attention because of their unique properties such as simple synthesis, easy labeling, good stability as well as excellent recognition and binding ability with target molecules [18, 19].

Gold nanomaterials with different nanostructures including spheres, rings, rods and cages were considered for modification of electrochemical sensors. Among them, gold nanorods have received a great attention sensing due to their unique optical properties concerning their aspect ratio (AR), for instance, faster electron transfer ability, higher surface area, and strong light scattering properties [20-25].

The aim of this work is to develop a highly sensitive electrochemical aptasensor based on gold nanorod for the determination of AFB1. The use of gold nanorods improves the electron transfer rate and provides high surface area for immobilization of aptamer. The fabricated aptasensor showed a good sensitivity, selectivity, as well as satisfactory results for the detection of AFB1 in real samples.

EXPERIMENTAL

Materials and reagents

Amino modified aptamer of AFB1 were purchased from Bioneer Co, South Korea. The sequence of nucleotides in the aptamer is shown below:

(5'-NH₂ modified) 5'-TGGGGTTTTGG TGGCG GTGGTGTACGGGCGAGG G-3'.

Sodium borohydride (NaBH₄), and cetyltrimethylammonium bromide (CTAB) were purchased from Sigma-Aldrich. Chloroauric acid (HAuCl₄·3H₂O) and silver nitrate (AgNO₃) was received from Merck. Ultrapure water obtained from the Millipore water purification system (Milli-Q, Millipore) was used for all solution preparation and all the other substances were analytical-reagent grade.

Apparatus

All electrochemical measurements, including cyclic voltammetry (CV), electrochemical impedance spectroscopy (EIS), and differential pulse voltammetry (DPV), were performed with A μ-AUTOLAB electrochemical system type III and FRA2 board computer controlled Potentiostat/Galvanostat (Eco-Chemie, Switzerland) driven with NOVA software in 2.5 mM Fe(CN)₆^{3-/4-} solution. A

conventional three electrode system was used for electrochemical measuring with Ag/AgCl (saturated KCl) electrode as the reference electrode, platinum wire as the counter electrode, and a bare or modified GC electrode (2 mm in diameter) as the working electrode.

Transmission electron microscopy (TEM) and scanning electron microscopy (SEM) images were recorded by a Hitachi H-800 electron microscope and Vega-Tescan electron microscope, respectively.

UV-Vis absorption spectrum of the synthesized Au nanorod was recorded using a VARIAN 300 Bio CARY UV-Vis spectrophotometer.

Synthesis of the Gold nanorods (Au-NRs)

Gold nanorods were prepared using seed-mediated growth method [26]. Seed solution was prepared in the following procedure: CTAB solution (5.0 mL, 0.20 M) was mixed with 5.0 mL of 0.0005 M HAuCl₄. To the stirred solution, 0.60 mL of freshly prepared ice-cold NaBH₄ 0.010 M was added. After mixing, the mixture was developed into a brownish yellow color solution. Vigorous stirring of the seed solution was continued for 2 min and kept at 25°C. For preparation of growth solution CTAB (5.0 mL, 0.20 M) was added to 70 μL of 0.004 M AgNO₃ solution at 25 °C and followed by adding 5.0 mL of 0.001 M HAuCl₄. After slow mixing of the solution 70 μL of 0.0788 M ascorbic acid was added. In the presence of ascorbic acid as a mild reducing agent the color of growth solution changed from dark yellow to colorless. Finally, 12.0 μL of as-prepared seed solution was added to the growth solution. The color of the solution gradually became colorless after vigorously stirring for 3 min. Then, the Au nanorod growth solution was left undisturbed for 12 h at 30°C. The Au nanorods were purified by centrifugation (10 000 rpm for 20 min) twice and redispersed into distilled water, and then sonicated for 30 min and stored for further use.

Fabrication of the sensor

The GC electrode was polished carefully with alumina powder (0.05 μm) on a soft polishing cloth, followed by rinsing thoroughly with doubly distilled water. In following, the surface of the electrode was coated by 10 μL of the synthesized Au nanorod and was kept at room temperature for 2 h. After rinsing with distilled water, 10 μL of the aptamer solution (1.0 μM) was incubated for 1 h on the modified electrode surface under humid

atmosphere condition. The electrode surface was rinsed with water to remove the excess unbound aptamer. The resultant electrode was denoted as Apt/Au-NRs/GCE and stored at 4°C for future use. The electrochemical experiment was carried out using different concentrations of AFB1 dropped on the surface of the electrode for 15 min incubation.

Electrochemical measurements

Electrochemical experiments were performed with μ -AUTOLAB electrochemical system. Cyclic voltammetry (CV), differential pulse voltammetry (DPV), and impedance measurements were carried out in a redox probe (0.1 M KCl containing 2.5 mM $\text{Fe}(\text{CN})_6^{3-/4-}$). The impedance spectra were measured in the frequency range from 10^5 to 1 Hz in a potential of 0.25 V versus Ag/AgCl (saturated KCl), with pulse amplitude of 50 mV and width of 50 ms.

Samples preparation

Noncontaminated rice was obtained from a local market. 5.0 g of the sample was extracted with 25 mL of the extraction solvent (80% methanol in the water) by shaking for 45 min. Then, the extract was separated from the insoluble materials by centrifugation for 10 min at 6000 rpm. The supernatant was diluted five times with the PBS (0.1M), and various concentrations of AFB1 were spiked to these samples. In the case of serum sample, the human serum sample was ordered from a local clinical laboratory and subjected to ultrafiltration by loading into a centrifugal filtration tube at 5000 rpm (30 min). Afterwards, the serum samples were diluted 5 times with PBS (0.1M), and different concentrations of AFB1 were spiked to these samples.

RESULTS AND DISCUSSION

Characterization of synthesized gold nanorods

The UV-Vis absorption property of the Au-NRs was investigated (Fig. 1A). Two typical absorption peaks of AuNRs were appeared in the UV-Vis spectrum. The related peaks to transverse and longitudinal surface plasmon resonance absorption were observed at 523 and 664 nm, respectively.

The morphology of the synthesized Au-NRs was characterized by TEM. Fig. 1B displays the TEM image of the Au-NRs confirming the formation of gold nanorods. Microscopic illustration was reflecting the formation of nanorods with the average length (L) about 50 nm and the width (W) about 20 nm.

Characterization of the aptasensor fabrication

The fabricated aptasensor was first characterized by cyclic voltammetry in 2.5 mM $\text{Fe}(\text{CN})_6^{3-/4-}$ solution. As shown in Fig. 2A, the Au-NRs/GCE (Fig. 2A-b) displayed more current than the bare GCE (Fig. 2A-a), which is attributed to the significant increase in the effective surface area of the electrode in the presence of Au-NRs resulting in facilitating the electron-transfer rate. Peak current decreased clearly after aptamer was assembled on the Au-NRs layer (Fig. 2A-c), indicating that the captured aptamer hindered the diffusion of ferricyanide toward the electrode surface.

EIS is an effective and powerful tool to study the surface property of the modified electrodes after each assembly. The impedance spectra consist of two parts: a high-frequency region as charge transfer resistance (R_{ct}), and a linear region at lower frequencies corresponding to the diffusion process. The Nyquist plots at bare GCE, Au-NRs/GCE, and Apt/Au-NRs/

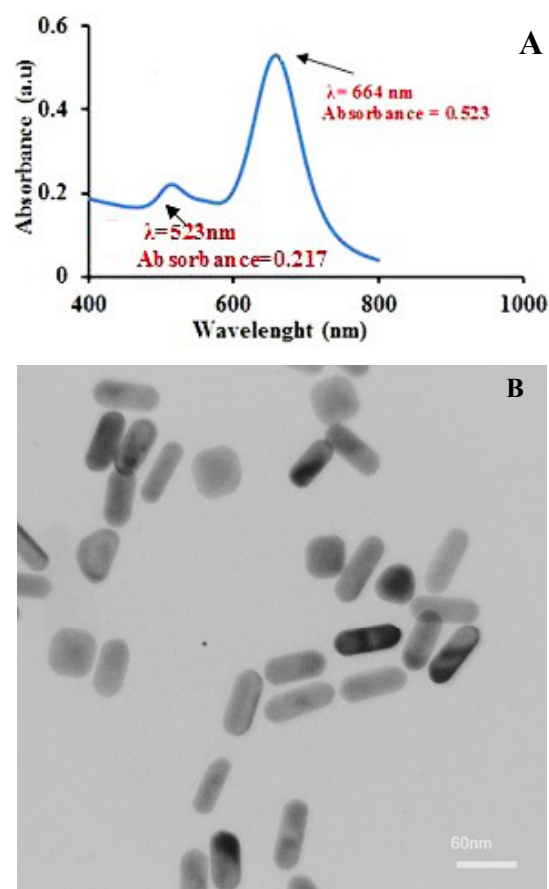


Fig. 1. (A) UV-Vis absorption spectrum of the synthesized Au-NRs. (B) TEM image of the synthesized Au-NRs.

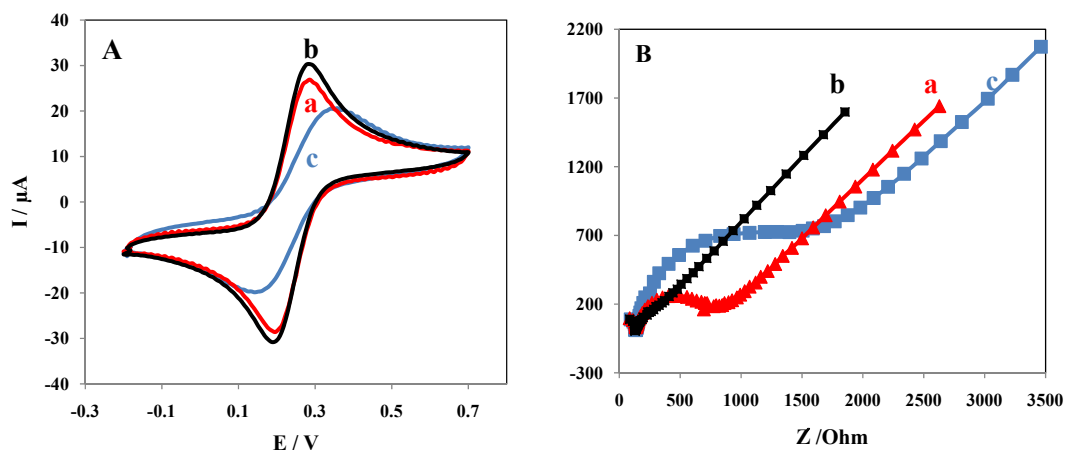


Fig. 2. (A) Cyclic voltammograms of 2.5 mM $[\text{Fe}(\text{CN})_6]^{3-/4-}$ at scan rate of 100 mV s^{-1} at (a) bare GCE, (b) Au-NRs/GCE, and (c) Apt/Au-NRs/GCE. (B) Nyquist plots of the EIS analysis in 2.5 mM $[\text{Fe}(\text{CN})_6]^{3-/4-}$ at (a) bare GCE, (b) Au-NRs/GCE, and (c) Apt/Au-NRs/GCE.

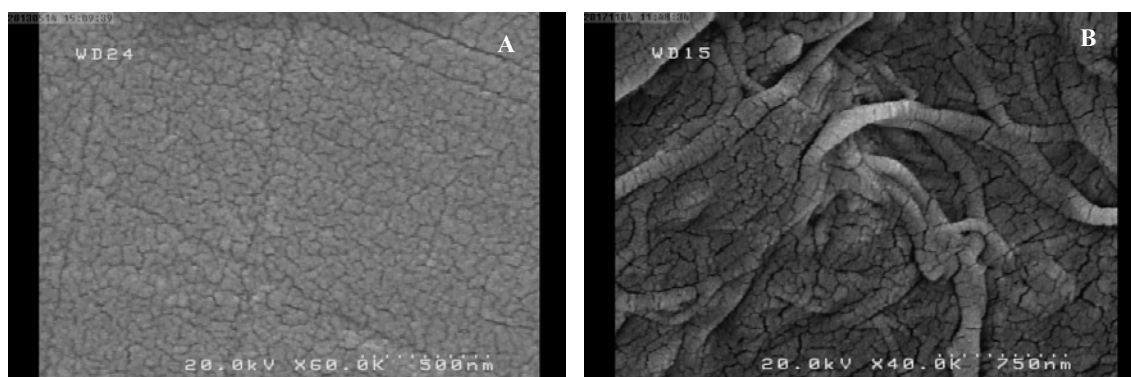


Fig. 3. SEM images of (A) bare, and (B) Au-NRs/GC electrodes.

GCE are shown in Fig. 2B. Compared with bare electrode, the modification of Au-NRs decreased the value of R_{ct} because of better electric conducting performance of gold nanorods. Immobilization of the aptamer led to an increase in the semi-circular diameter which could be due to the presence of phosphate/phosphonate groups of aptamer that repelled the negatively charged redox probes ($\text{Fe}(\text{CN})_6^{3-/4-}$) anions and thus increased the R_{ct} .

The modification of electrode was further verified by studying the surface morphology of the electrode. The SEM image of the bare electrode, Fig. 3A, shows a smooth and uniform surface. Nanorods obviously were seen in SEM image of Au-NRs/GCE (Fig. 3B).

Optimization of incubation time for salmonella detection

To obtain excellent analytical performances of

the prepared aptasensor, aptamer incubation time, aptamer concentration, and AFB1 incubation time were optimized by the use of DPV. The incubation time of aptamer is an important parameter affecting the analytical performance of the constructed aptasensor. Experiments were carried out with varying incubation times from 10 to 240 min. The results showed that the response is increased by increasing the incubation times until 160 min and after that by increasing the incubation times the response remains almost constant (Fig. 4A). Thus, an incubation time of 4 h was chosen as the optimal time. The concentration of aptamer is another important parameter affecting the response greatly. To optimize this parameter, various aptamer concentrations of 0.1 - 4.0 μM during the fabrication of the aptasensor were examined. The signal of the aptasensor fabricated with 1.0 μM concentration was close to the saturation level of the current

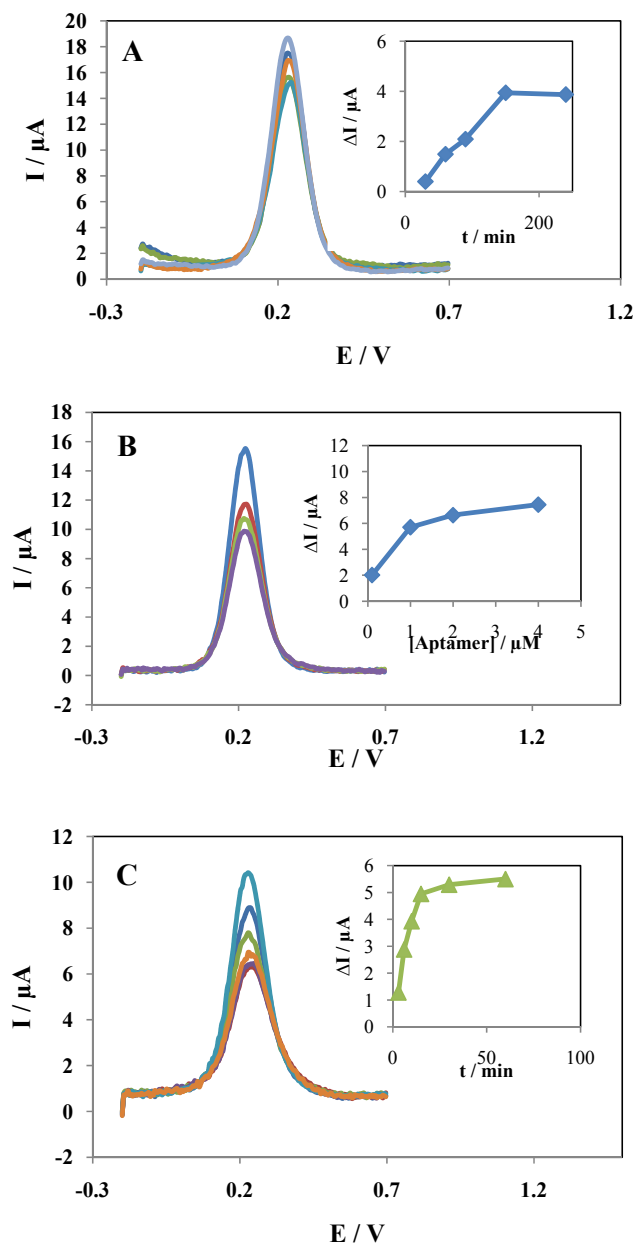


Fig. 4. A, B and C are the DPV responses of the aptasensor in 2.5 mM $[\text{Fe}(\text{CN})_6]^{3/4-}$ for three variables including various incubation times of aptamer, various aptamer concentration and various incubation times of AFB1, respectively. The insets show the variation of ΔI vs. the mentioned variables.

response, and thus 1.0 μM aptamer was applied for the sensor fabrication (Fig. 4B). Incubation time of AFB1 with aptamer is one of the most important parameters affecting the performances of the aptasensor. The results showed that the current response increases gradually until 15 min and remains stable thereafter, indicating that the specific binding interaction between aptamers and

AFB1 reaches saturation. So, 15 min was chose as the optimal condition for AFB1 detection (Fig. 4C).

Analytical performance of the aptasensors

After the above optimizations, the responses of the aptasensor for different concentrations of AFB1 were examined using the DPV technique. The typical DPV of aptasensor, shown in Fig.

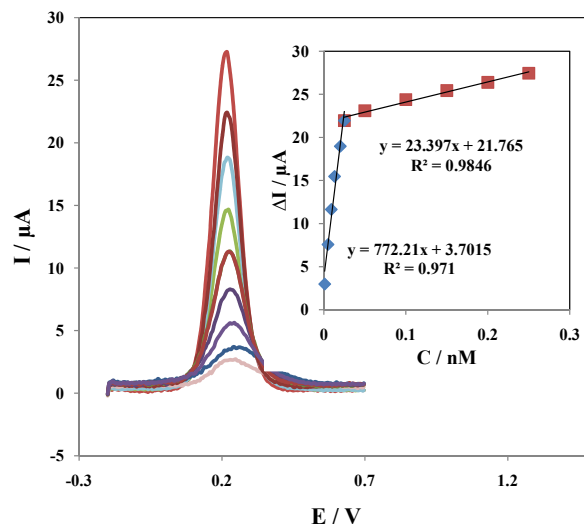


Fig. 5. (A) DPV responses of the aptasensor in 2.5 mM $[\text{Fe}(\text{CN})_6]^{3-/4-}$ after incubation with 0.001, 0.005, 0.009, 0.013, 0.02, 0.025, 0.05, 0.1, 0.15, 0.2 and 0.25 nM of AFB1.

Inset) calibration curve for AFB1 aptasensor. The DPV measurements are performed from -0.2 to 0.7 V, with amplitude of 50 mV and a pulse width of 50 ms.

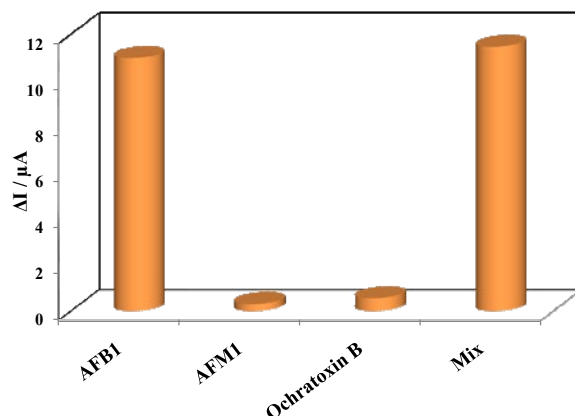


Fig. 6. Selectivity study of the aptasensor.

5, shows that by increasing AFB1 concentration the peak current decreases. This means that the aptamer was folded and formation of AFB1-aptamer complexes on the sensing interface caused inhibition of electron transfer of redox probe $(\text{Fe}(\text{CN})_6^{3-/4-})$. Sensitive quantitative detection of AFB1 was carried out by monitoring the decrease of DPV responses of $(\text{Fe}(\text{CN})_6^{3-/4-})$ peak current by increasing the AFB1 concentration. The calibration curve for AFB1 detection under optimal conditions gave two linear ranges from 0.001 to 0.025 nM by regression equation $\Delta I (\mu\text{A}) = 772.21 [\text{AFB1}] (\text{nM}) + 3.7015$ ($R^2 = 0.971$) and from 0.025 nM to 0.25 nM by regression equation $\Delta I (\mu\text{A}) = 23.397 [\text{AFB1}]$

(nM) + 21.765 ($R^2 = 0.9846$) (Fig. 5). The obtained limit of detection was 0.3 pM (a signal-to-noise ratio of 3). In addition, the analytical performance of the aptasensor in terms of the LOD and linear concentration range is comparable or even better than that of some recent studies (Table 1).

Selectivity, stability and reproducibility of the aptasensor

The selectivity is another important issue for the fabrication of sensor. In order to evaluate the selectivity of the aptasensor, it was incubated with 20 pM AFB1 and 100-fold interfering compounds, ochratoxin B and AFM1. As shown in Fig. 6, a

Table 1. Comparison of the sensitivity of currently available methods for the detection of AFB1.

Method	LOD	Reference
Electrochemical indirect ELISA with pulse voltammetry detection	0.096 nM	[27]
Chemiluminescence competitive aptamer assay	0.35 nM	[28]
UHPLC-FLD	2.0 ng mL ⁻¹	[29]
Enzyme immunoassay	2.0 ng mL ⁻¹	[30]
Apt/Au-NRs/GCE	0.3 pM	This work

Table 2. Recoveries of AFB1 in the real samples for applicability of aptasensor in a real matrix (n=3).

Real Sample	Spiked AFB1 μM	Found AFB1 μM	% Recovery	% RSD
rice	0.100	0.097	97	2.175
	0.200	0.195	97.5	3.845
serum	0.100	0.095	95	3.256
	0.200	0.213	106.5	4.215

significant current response was observed when the aptasensor was incubated with AFB1 and mixed solution, whereas the incubation of the aptasensor with other interferences showed no detectable change of DPV signals, indicating that developed aptasensor was highly specific toward AFB1.

The repeatability of the aptasensor was evaluated by analyzing 10 pM AFB1 with six electrodes. The relative standard deviation (RSD) of the measurements of constant concentration of AFB1 for the six electrodes was 2.32%, suggesting the suitable repeatability of the offered aptasensor. Moreover, about 96.46% and 91.62% of the initial response of the sensor for 10 pM AFB1 were remained after being stored at 4°C for 1 week and 4 weeks, respectively, which indicates a good stability of the aptasensor. Thus, the developed aptasensor provides an appropriate tool for the detection of AFB1.

The reproducibility of the proposed aptasensor is evaluated by analyzing the certain amount of AFB1 by six aptasensors, which the relative standard deviation was achieved 2.51%, demonstrating the acceptable reproducibility of the proposed aptasensor.

Analysis of rice and serum samples

To verify the applicability of the fabricated sensor for real sample analysis, the as-prepared sensor was used to study real samples using spiked human serum and rice samples. The solutions of extraction samples were added with AFB1 standard solution at three different concentrations (1.0, 5.0, 20.0 pM). Table 2 shows the results of recovery testing ranging from 95.0% to 106.5%, indicating

the excellent reliability of the developed biosensor for the detection of AFB1 in real samples.

CONCLUSION

This study describes a sensitive and selective aptasensor for detection of AFB1, involving aptamer as specific recognition element and gold nanorods as a sensing interface. Fabricated aptasensor showed a suitable sensitivity towards AFB1 determination in a wide range of concentrations, from 1.0 pM to 0.25 nM with the limit of detection as 0.3 pM by means of DPV, while common interferences such as aflatoxin M1, ochratoxin A, ochratoxin B did not show any significant signal. In addition, the aptasensor provided good precision, reproducibility, regeneration and storage stability, and satisfactory accuracy for determination of AFB1 in real samples.

CONFLICT OF INTEREST

The authors declare that there is no conflict of interests regarding the publication of this manuscript.

REFERENCES

- [1] Deng G, Xu K, Sun Y, Chen Y, Zheng T, Li J. High Sensitive Immunoassay for Multiplex Mycotoxin Detection with Photonic Crystal Microsphere Suspension Array. *Analytical Chemistry*. 2013;85(5):2833-40.
- [2] Saremi H, Okhovvat SM. Mycotoxin producing *Fusarium* species associated with plant disease on potato, wheat, corn and animal diseases in northwest Iran. *Commun Agric Appl Biol Sci*. 2006; 71(3 Pt B): 1175-85.
- [3] Li P, Zhang Q, Zhang W, Zhang J, Chen X, Jiang J, et al. Development of a class-specific monoclonal antibody-based ELISA for aflatoxins in peanut. *Food Chemistry*. 2009;115(1):313-7.

- [4] Lv X, Li Y, Cao W, Yan T, Li Y, Du B, et al. A label-free electrochemiluminescence immunosensor based on silver nanoparticle hybridized mesoporous carbon for the detection of Aflatoxin B1. *Sensors and Actuators B: Chemical*. 2014;202:53-9.
- [5] McKean C, Tang L, Billam M, Tang M, Theodorakis CW, Kendall RJ, et al. Comparative acute and combinative toxicity of aflatoxin B1 and T-2 toxin in animals and immortalized human cell lines. *Journal of Applied Toxicology*. 2006;26(2):139-47.
- [6] Kolosova AY, Shim W-B, Yang Z-Y, Eremin SA, Chung D-H. Direct competitive ELISA based on a monoclonal antibody for detection of aflatoxin B1. Stabilization of ELISA kit components and application to grain samples. *Analytical and Bioanalytical Chemistry*. 2005;384(1):286-94.
- [7] Lee NA, Wang S, Allan RD, Kennedy IR. A Rapid Aflatoxin B1 ELISA: Development and Validation with Reduced Matrix Effects for Peanuts, Corn, Pistachio, and Soybeans. *Journal of Agricultural and Food Chemistry*. 2004;52(10):2746-55.
- [8] Xu G, Zhang S, Zhang Q, Gong L, Dai H, Lin Y. Magnetic functionalized electrospun nanofibers for magnetically controlled ultrasensitive label-free electrochemiluminescent immune detection of aflatoxin B1. *Sensors and Actuators B: Chemical*. 2016;222:707-13.
- [9] Linting Z, Ruiyi L, Zaijun L, Qianfang X, Yinjun F, Junkang L. An immunosensor for ultrasensitive detection of aflatoxin B1 with an enhanced electrochemical performance based on graphene/conducting polymer/gold nanoparticles/the ionic liquid composite film on modified gold electrode with electrodeposition. *Sensors and Actuators B: Chemical*. 2012;174:359-65.
- [10] Dohnal V, Dvořák V, Malíř F, Ostrý V, Roubal T. A comparison of ELISA and HPLC methods for determination of ochratoxin A in human blood serum in the Czech Republic. *Food and Chemical Toxicology*. 2013;62:427-31.
- [11] Entwisle AC, Williams AC, Mann PJ, Slack PT, Gilbert J. Liquid Chromatographic Method with Immunoaffinity Column Cleanup for Determination of Ochratoxin A in Barley: Collaborative Study. *Journal of AOAC International*. 2000; 83(6): 1377-83.
- [12] Soleas GJ, Yan J, Goldberg DM. Assay of Ochratoxin A in Wine and Beer by High-Pressure Liquid Chromatography Photodiode Array and Gas Chromatography Mass Selective Detection. *Journal of Agricultural and Food Chemistry*. 2001;49(6):2733-40.
- [13] Privett BJ, Shin JH, Schoenfisch MH. Electrochemical Sensors. *Analytical Chemistry*. 2008;80(12):4499-517.
- [14] Bakker E, Qin Y. Electrochemical Sensors. *Analytical Chemistry*. 2006;78(12):3965-84.
- [15] Bao W-J, Yan Z-D, Wang M, Zhao Y, Li J, Wang K, et al. Distance-determined sensitivity in attenuated total reflection-surface enhanced infrared absorption spectroscopy: aptamer-antigen compared to antibody-antigen. *Chemical Communications*. 2014;50(58):7787.
- [16] Yu P, Zhou J, Wu L, Xiong E, Zhang X, Chen J. A ratiometric electrochemical aptasensor for sensitive detection of protein based on aptamer-target-aptamer sandwich structure. *Journal of Electroanalytical Chemistry*. 2014;732:61-5.
- [17] Wu D, Ren X, Hu L, Fan D, Zheng Y, Wei Q. Electrochemical aptasensor for the detection of adenosine by using PdCu@MWCNTs-supported bienzymes as labels. *Biosensors and Bioelectronics*. 2015;74:391-7.
- [18] Emrani AS, Danesh NM, Lavaee P, Ramezani M, Abnous K, Taghdisi SM. Colorimetric and fluorescence quenching aptasensors for detection of streptomycin in blood serum and milk based on double-stranded DNA and gold nanoparticles. *Food Chemistry*. 2016;190:115-21.
- [19] Wang B, Chen Y, Wu Y, Weng B, Liu Y, Lu Z, et al. Aptamer induced assembly of fluorescent nitrogen-doped carbon dots on gold nanoparticles for sensitive detection of AFB1. *Biosensors and Bioelectronics*. 2016;78:23-30.
- [20] Zhu C, Peng H-C, Zeng J, Liu J, Gu Z, Xia Y. Facile Synthesis of Gold Wavy Nanowires and Investigation of Their Growth Mechanism. *Journal of the American Chemical Society*. 2012;134(50):20234-7.
- [21] Langille MR, Personick ML, Zhang J, Mirkin CA. Defining Rules for the Shape Evolution of Gold Nanoparticles. *Journal of the American Chemical Society*. 2012;134(35):14542-54.
- [22] Wang Y, Black KCL, Luehmann H, Li W, Zhang Y, Cai X, et al. Comparison Study of Gold Nanohexapods, Nanorods, and Nanocages for Photothermal Cancer Treatment. *ACS Nano*. 2013;7(3):2068-77.
- [23] Huang X, Neretina S, El-Sayed MA. Gold Nanorods: From Synthesis and Properties to Biological and Biomedical Applications. *Advanced Materials*. 2009;21(48):4880-910.
- [24] Rex M, Hernandez FE, Campiglia AD. Pushing the Limits of Mercury Sensors with Gold Nanorods. *Analytical Chemistry*. 2006;78(2):445-51.
- [25] Han X, Fang X, Shi A, Wang J, Zhang Y. An electrochemical DNA biosensor based on gold nanorods decorated graphene oxide sheets for sensing platform. *Analytical Biochemistry*. 2013;443(2):117-23.
- [26] Nikoobakht B, El-Sayed MA. Preparation and Growth Mechanism of Gold Nanorods (NRs) Using Seed-Mediated Growth Method. *Chemistry of Materials*. 2003;15(10):1957-62.
- [27] Piermarini S, Micheli L, Ammida NHS, Pallechi G, Moscone D. Electrochemical immunosensor array using a 96-well screen-printed microplate for aflatoxin B1 detection. *Biosensors and Bioelectronics*. 2007;22(7):1434-40.
- [28] Shim W-B, Mun H, Joung H-A, Ofori JA, Chung D-H, Kim M-G. Chemiluminescence competitive aptamer assay for the detection of aflatoxin B1 in corn samples. *Food Control*. 2014;36(1):30-5.
- [29] Corcuera L-A, Ibáñez-Vea M, Vettorazzi A, González-Peñas E, Cerain ALD. Validation of a UHPLC-FLD analytical method for the simultaneous quantification of aflatoxin B1 and ochratoxin A in rat plasma, liver and kidney. *Journal of Chromatography B*. 2011;879(26):2733-40.
- [30] Saha D, Acharya D, Roy D, Shrestha D, Dhar TK. Simultaneous enzyme immunoassay for the screening of aflatoxin B1 and ochratoxin A in chili samples. *Analytica Chimica Acta*. 2007;584(2):343-9.